Molecular Biology of the Cell
Vol. 10, 1061–1075, April 1999

Sla1p Is a Functionally Modular Component of the Yeast Cortical Actin Cytoskeleton Required for Correct Localization of Both Rho1p-GTPase and Sla2p, a Protein with Talin Homology

Kathryn R. Ayscough,*† Jennifer J. Eby,‡ Thomas Lila,‡ Hilary Dewar,* Keith G. Kozminski,‡ and David G. Drubin‡

*Department of Biochemistry, University of Dundee, Dundee DD1 5EH, Scotland, United Kingdom; and ‡Department of Molecular and Cell Biology, University of California, Berkeley, California 94720

Submitted November 23, 1998; Accepted February 1, 1999
Monitoring Editor: Thomas D. Pollard

SLA1 was identified previously in budding yeast in a genetic screen for mutations that caused a requirement for the actin-binding protein Abp1p and was shown to be required for normal cortical actin patch structure and organization. Here, we show that Sla1p, like Abp1p, localizes to cortical actin patches. Furthermore, Sla1p is required for the correct localization of Sla2p, an actin-binding protein with homology to talin implicated in endocytosis, and the Rho1p-GTPase, which is associated with the cell wall biosynthesis enzyme β-1,3-glucan synthase. Mislocalization of Rho1p in *sla1* null cells is consistent with our observation that these cells possess aberrantly thick cell walls.

Expression of mutant forms of Sla1p in which specific domains were deleted showed that the phenotypes associated with the full deletion are functionally separable. In particular, a region of Sla1p encompassing the third SH3 domain is important for growth at high temperatures, for the organization of cortical actin patches, and for nucleated actin assembly in a permeabilized yeast cell assay. The apparent redundancy between Sla1p and Abp1p resides in the C-terminal repeat region of Sla1p. A homologue of *SLA1* was identified in *Schizosaccharomyces pombe*. Despite relatively low overall sequence homology, this gene was able to rescue the temperature sensitivity associated with a deletion of *SLA1* in *Saccharomyces cerevisiae*.

INTRODUCTION

The actin cytoskeleton in eukaryotic cells plays a central role in the generation of polarity and determination of cell morphology. In yeast, as in other eukaryotes, the organization of the actin cytoskeleton is regulated by several classes of actin-binding proteins. The actions of these proteins are crucial for the timing and position of cortical actin assembly, which is essential for bud and mating projection formation. Representatives of most classes of actin-binding protein have been identified in *Saccharomyces cerevisiae*, and their importance to actin function has been demonstrated genetically. Many of the proteins, including profilin, tropomyosin, fimbrin, and cofilin, behave in vitro in a similar manner to their homologs from other organisms (reviewed by Welch *et al.*, 1994; Ayscough, 1998).

Yeast Abp1 was identified as an actin-binding protein by affinity chromatography on an actin column (Drubin *et al.*, 1988). It was localized to the cortical actin patches of yeast cells, and its overexpression was shown to lead to severe defects in the actin cytoskeleton and depolarized cell growth; however, deletion of the *ABP1* gene had no readily observable phenotype. A synthetic lethal screen identified mutations that caused cells to require expression of *ABP1* (Holtzman *et al.*, 1993). This approach lead to the isolation of three genes. One of these was the previously identified

† Corresponding author. E-mail address: kayscough@bad.dundee.ac.uk.

SAC6, which encodes yeast fimbrin, an actin-bundling protein. The other two genes were previously unknown and were called *SLA1* and *SLA2* for synthetically lethal with *ABP1. SLA1* was cloned and sequenced and shown to encode a protein with an interesting set of structural elements. In its N-terminal third it contains three SH3 domains. In various organisms, SH3 domains have been shown to mediate protein–protein interactions of signaling and cytoskeletal proteins (Pawson and Gish, 1992; Mayer and Eck, 1995). The central third of Sla1p contains a putative SH3-domain binding consensus (Ren *et al.*, 1993; Yu *et al.*, 1994), and its C-terminal third is composed of 26 repeats with an approximate consensus TGGXXXPQ. This consensus repeat has homology to repeats in a range of proteins including the yeast protein Pan1p, a protein that has itself been postulated to be involved in organization of the actin cytoskeleton (Tang and Cai, 1996) and sea urchin sperm bindins (Gao *et al.*, 1986; Minor *et al.*, 1991), and also to the major plant structural proteins wheat glutenin and barley hordeins (Field *et al.*, 1987; Halford *et al.*, 1992).

Deletion of *SLA1* caused cells to be temperature sensitive and to exhibit defects in their cortical actin cytoskeletons. Rather than the wild-type situation in which the cortical actin is organized as many small actin patches that are highly polarized, *sla1* null cells had fewer cortical "chunks" of actin that appeared larger than normal and were not as well polarized (Holtzman *et al.*, 1993). *sla1* null cells also showed increased resistance to the actin-disrupting drug latrunculin-A (Ayscough *et al.*, 1997). In this article, we demonstrate by immunolocalization of Sla1p that it is a component of the cortical actin patches. We show that Sla1p plays a critical role in proper localization of two proteins, Sla2p and the small GTP-binding protein Rho1p, and in the spatial control of cell wall biosynthesis. Using deletion analysis, we then address the role of structural domains within the protein, using both in vivo and in vitro approaches, and show that Sla1p is a multifunctional protein with different functions that are attributable to distinct domains.

MATERIALS AND METHODS

Materials

Unless stated otherwise, chemicals were obtained from Sigma (St. Louis, MO) or Fisher (Pittsburgh, PA). Reagents for molecular biology were obtained from New England Biolabs (Beverly, MA).

Yeast Strains and Growth Conditions

Yeast strains used in this study are listed in Table 1. Unless stated otherwise, cells were grown with rotary shaking at 25°C in liquid YPD medium (1% yeast extract, 2% bacto peptone, 2% glucose), except for plasmid-carrying strains, which were grown on synthetic medium with appropriate selection as described by Kaiser *et al.* (1994). For testing *ABP1* dependence, cells were plated on synthetic medium containing 1 mg/ml 5-fluororotic acid (5-FOA). Culture density was measured using a hemocytometer and by measuring turbidity at 600 nm. Transformation of yeast was performed using lithium acetate as described (Kaiser *et al.*, 1994).

Table 1. Yeast strains used in this study

Strain	Genotype
KAY40	*MAT***a**/α *ura3-52/ura3-52*
KAY14	*MAT***a**/α *ura3-52/ura3-52 his3-*Δ*200/his3-*Δ*200* Δ*sla1*::*URA3*/Δ*sla1*::*URA3*
KAY78	*MAT* α *his3-*Δ*200 leu2-3,112 ura3-52,* Δ*abp1*::*LEU2 sla1-1* [pDD13: *URA3 CEN, ABP1*]
DDY664	*MAT***a** *ura3-52 leu2-3,112 lys2-801am*
DDY757	*MAT***a** *cry1 ade2-1 his3-11,15 leu2-3,112 ura3-1 trp1-1 can1-100*
DDY1097	*MAT***a** *cry1 ade2-1 his3-11,15 leu2-3,112 ura3-1 trp1-1 can1-100* [pRS313 + *GAL10–RHO1*]
DDY1098	*MAT***a** *cry1 ade2-1 his3-11,15 leu2-3,112 ura3-1 trp1-1 can1-100* [pRS313]

For the galactose-induced overexpression of Rho1p, strain DDY757 was transformed with pRS313 (Sikorski and Hieter, 1989) containing no insert or the galactose-inducible *GAL10* promoter fused to *RHO1* (gift of Dr. Alan Myers, Iowa State University), yielding strains DDY1098 and DDY1097, respectively. Log-phase transformant cultures were washed into rich medium containing 2% raffinose (wt/vol) as the sole carbon source. Galactose was then added to 2% raffinose (wt/vol) 12 h later; incubation then continued for another 8 h before the cells were harvested.

Cloning Procedures

SLA1 was cloned as a *Sal*I fragment from one of the original plasmids isolated in the synthetic lethal screen of Holtzman *et al.* (1993). Plasmid constructions are listed in Table 2. In vitro mutagenesis was performed using the Stratagene Quick Change Kit (Stratagene, La Jolla, CA). All mutations were verified by sequencing. The *Schizosaccharomyces pombe* cosmid was obtained from The Sanger Center (Hinxton, UK).

Myc tagging of Las17p/Bee1p and Sla1p was performed using PCR-based homologous recombination (Baudin *et al.*, 1993). The selectable marker was *Kluyveromyces lactis TRP1*, and the plasmid used for generating the 9 × myc tag was a generous gift from K. Nasmyth (Imp, Vienna, Austria).

Antibody Production and Affinity Purification

Polyclonal antibodies to Sla1p were raised against a fusion of amino acids 854–920 to the C-terminus of glutathione *S*-transferase. Fusion proteins were generated using the protocol from Pharmacia (Piscataway, NJ) and finally eluted from glutathione-Sepharose beads using reduced glutathione. The eluted proteins were used to raise antisera in New Zealand White rabbits. Antisera obtained after the third injection of antigen were affinity-purified on a cyanogen bromide-activated Sepharose-B column (Pharmacia) with the glutathione *S*-transferase–fusion protein bound.

Rho1p and Cdc42p antibodies were raised against synthetic peptides conjugated to rabbit serum albumin (RSA). Production of Cdc42 antibody, raised against the *S. cerevisiae* Cdc42 peptide QRQRLRPITSEQGSRL, is fully described elsewhere (Kozminski, Chen, Rodal, and Drubin, unpublished observations). To prepare RSA as a carrier for Rho1 peptide, 0.8 mg of the heterobifunctional cross-linker 4-(p-maleimidophenyl) butyric acid *N*-hydroxy-succinimide ester (Sigma) were dissolved in 75 μl of dimethylformamide; this solution was then added with continuous stirring to a Wheaton V-vial (VWR, San Francisco, CA) containing 2 mg of RSA dissolved

Table 2. Plasmids constructed in this study

Plasmid name	Construction
pKA50	pRS313 (CEN, HIS3) was cut with *Pvu*II and religated to remove polylinker.
pKA51	*SLA1* on *Sal* I fragment was blunt-ended using Klenow and ligated into pKA50 at the *Pvu* II site.
pKA53	pKA51 was cut with *Eco* RI removing a 1182-bp fragment and religated.
pKA54	PCR was used to generate an *Apa* I site at base 9 of the *SLA1* coding sequence in pKA51. The plasmid was then cut with *Apa* I releasing a 575-bp fragment encompassing the first two SH3 domains.
pKA55	PCR was used to generate a *Bam* HI site at base 1522 of the *SLA1* coding sequence in pKA51. The plasmid was then cut with *Bam* HI releasing a 1495-bp fragment encompassing the central "gap2" region.
pKA13	pKA51 was cut with *Bam* HI and *Eag* I, blunt-ended, and religated releasing a 754-bp fragment encoding most of the C-terminal repeat region.
pKA116	*Xho* I sites were generated by in vitro mutagenesis on either side of the third SH3 domain in pKA51. This domain was then excised, and the plasmid was religated.
pKA128	In vitro mutagenesis was used to mutate the coding sequence for the proline helix motif to give a change of P to S at residue 626.
pKA129	*Xho* I sites were generated by in vitro mutagenesis on the 5′ side of the coding region for the third SH3 domain and on the 3′ side of the second SH3 domain in pKA51. This Gap1 domain was then excised, and the plasmid was religated giving *Sla1*-Δgap1.
pKA130	*Xho* I sites were generated by in vitro mutagenesis on either side of the third SH3 domain in pKA54. This domain was then excised, and the plasmid was religated giving *Sla1*-Δall SH3.
pKA32	The DNA coding for the mutant *Sla1*-ΔG1+SH3#3 was excised from pKA53 using *Xba* I and cloned into pRS316 (CEN, URA3).
pKA139	*S. pombe* cosmid SPAC16E8 was cut with *Eco* RI and *Hpa* I, and the relevant fragment was cloned into pRS423 (2μ, HIS3).

in 50 μl of deionized water. An additional 25 μl of dimethylformamide were added to clarify the solution. After incubation at room temperature for 30 min, unreacted 4-(p-maleimidophenyl) butyric acid *N*-hydroxy-succinimide ester was removed by two sequential gel filtrations through 1-ml Sephadex G-25 (Pharmacia) spin columns equilibrated with 0.1 M Na phosphate buffer (pH 6.5). To reduce the salt concentration, the eluate (200 μl) was diluted fourfold with deionized water. The peptide MSQQVGNSIRRKGC, which contains the N-terminal residues of *S. cerevisiae* Rho1p (underlined), was synthesized by Dr. David King (University of California, Berkeley). Two milligrams of Rho1p peptide were dissolved in 80 μl of deionized water followed by the gradual addition of 20 μl of 0.1 M Na phosphate buffer (pH 6.5) containing 2 mM EDTA. The peptide solution was then added dropwise (10 μl) with constant stirring to the 4-(p-maleimidophenyl) butyric acid *N*-hydroxy-succinimide ester-RSA solution. Cross-linking of the Rho1p peptide via the C-terminal cysteine proceeded for 3 h at room temperature. To remove unreacted peptide, the reaction was then dialyzed overnight against 2 l of deionized water at 4°C using No. 7 Spectra/Por (MWCO 1000) dialysis tubing (VWR). The dialysate was aliquoted and stored frozen at −20°C. Protein concentration of the dialysate was determined by a Bradford protein assay (Bio-Rad, Hercules, CA). New Zealand White rabbits were injected subcutaneously with peptide. Immunogenicity against Rho1p was first detected in yeast whole-cell extracts at week 14.

Rho1p antibody was affinity-purified using a Rho1p peptide column. By vacuum filtration, 0.4 g of divinylsulfone (4% cross-linked) agarose was hydrated with deionized water and sequentially washed once with 1.0 M Na phosphate buffer (pH 6.5), twice with 0.5 M Na carbonate buffer (pH 10), once with deionized water, and once with coupling buffer (10 mM Na phosphate buffer, pH 6.5, 2.5 mM EDTA). Two milligrams of Rho1 peptide were dissolved in 200 μl of coupling buffer and added to 1 ml of washed divinylsulfone agarose in a microcentrifuge tube. The tube was flushed with N_2. C-terminal–coupling of the peptide to the agarose proceeded for 48 h at room temperature with gentle rocking. Unreacted vinyl groups were blocked by the addition of 5 μl of β-mercaptoethanol followed by an additional 3-h incubation. Coupling buffer was removed by several washes with PBS. Preparation of the affinity column and elution of bound antibody were performed as described (Kozminski, Chen, Rodal, and Drubin, unpublished data).

Immunoblotting Procedures

Yeast whole-cell lysates were prepared as described by Belmont and Drubin (1998) and run on 13% polyacrylamide gels for Rho1p and tubulin immunoblotting or on 7.5% gels for Sla1p blots. For immunoblots, affinity-purified rabbit anti-yeast Rho1p peptide antibody was diluted 1:500, rabbit anti-yeast β-tubulin antibody 206 (Bond *et al.*, 1986) was diluted 1:20,000, and rabbit anti-yeast Sla1p was diluted 1:250. To specifically block Rho1p antibody, affinity-purified Rho1p antibody was diluted 100-fold into 1 ml of Tris-buffered saline containing 1 mg of Rho1p peptide and incubated overnight at 4°C. Detection of antibody binding was performed using an enhanced chemiluminescence kit from Amersham (Arlington Heights, IL).

Fluorescence Microscopy Procedures and Permeabilized Cell Assays

Rhodamine–phalloidin (Rd–phalloidin) staining of actin was performed as described by Pringle *et al.* (1989). Cells were processed for immunofluorescence microscopy essentially as described by Pringle *et al.* (1991) and by Ayscough and Drubin (1997). The cold methanol/acetone step (Pringle *et al.*, 1991) was required to observe actin, Abp1p, Arp2p, cofilin, calmodulin, Srv2p, Sla2p, and Spa2p. To visualize Las17p/Bee1p, Cdc42p, Rho1p, and Sla1p, the methanol/acetone step was replaced with an incubation of the cells in 0.2% SDS in PBS for 5 min. Primary antibodies were raised to the particular proteins except for Las17p/Bee1p, which was myc-tagged and then localized using polyclonal antiserum A14 against the myc epitope (Santa Cruz Biotechnology, Santa Cruz, CA). The primary antibodies to actin, Abp1p, cofilin, Sla2p, Cdc42p, Sla1p, and Rho1p, were generated in the laboratory of D.D. Other antibodies were gifts: anti-Arp2p from B. Winsor (Université Louis Pasteur, Strasbourg, France) (Moreau *et al.*, 1996); anti-Srv2p from J. Field (University of Pennsylvania, Philadelphia, PA) (Freeman *et al.*, 1996); anti-calmodulin from M. Stark (University of Dundee, Dundee, Scotland) (Brockerhoff and Davis, 1992; Stirling *et al.*, 1994); and anti-Spa2p from M. Snyder (Yale University, New Haven, CT) (Snyder, 1989). Secondary antibodies used were FITC-conjugated goat anti-guinea pig IgG (Cappell/Organon Technika, Malvern, PA) at a

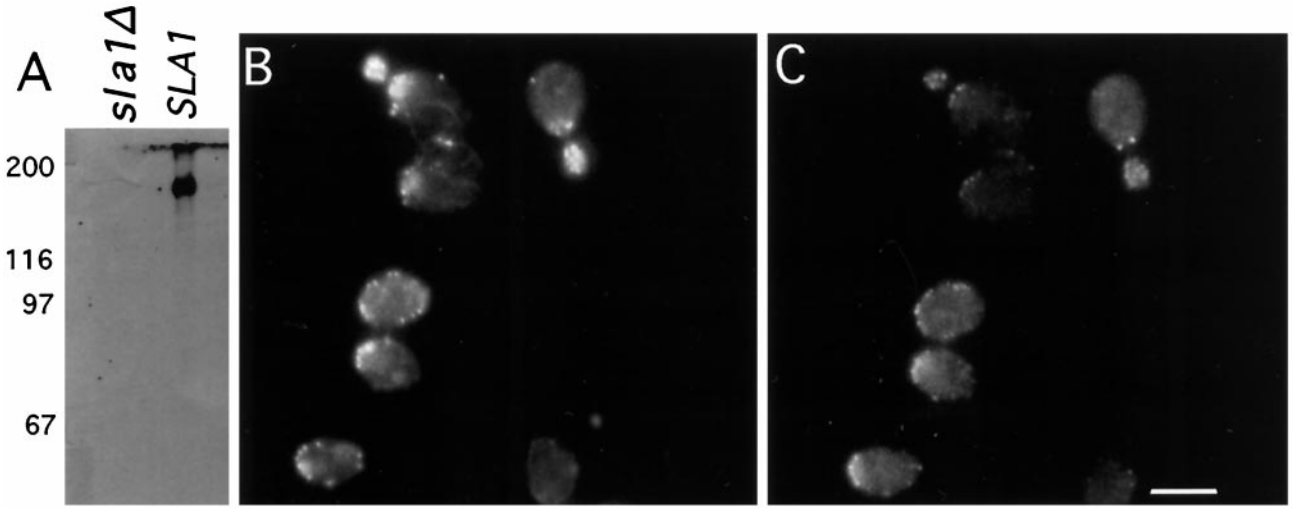

Figure 1. Localization of Sla1p and actin using indirect double-label immunofluorescence microscopy. (A) Antibodies raised to Sla1p were used to detect Sla1p on Western blots of wild-type cells and to demonstrate lack of reactive proteins in *sla1* null cells. (B and C) Immunofluorescence microscopy was then performed to localize Sla1p (C) and actin (B) in wild-type diploid cells. Bar, 5 μm.

dilution of 1:1000 and CY3-conjugated sheep anti-rabbit IgG (Sigma) at a dilution of 1:200.

The permeabilized cell assay was performed essentially as described (Li *et al.*, 1995). In addition, the effect of adding cell extracts before incubation was tested to examine whether Sla1p in such extracts was able to reconstitute the actin-assembly activity that was absent in *SLA1* null mutants. Extracts were prepared from late log-phase cells that had been lysed by the liquid nitrogen grinding method (Sorger and Pelham, 1987). After the grinding step, an equal volume of buffer (50 mM K-HEPES, pH 7.5, 100 mM KCl, 3 mM $MgCl_2$, 1 mM EGTA) was added, and the lysate was spun at 100,000 $\times$ *g* for 60 min. The resulting high speed supernatant was used in the assays at a concentration of 20 mg/ml.

Cells were viewed with an Olympus BX-60 fluorescence microscope (Olympus, Lake Success, NY) with a 100 W mercury lamp and an Olympus 100X Plan–NeoFluar oil immersion objective. Images were captured electronically using a Sys3000 cooled charge-coupled device camera (Digital Pixel Advanced Imaging Systems, Brighton, UK) and displayed on an Apple Macintosh computer using IP lab software (Scanalytics, Fairfax, VA). Quantitation of fluorescence for the permeabilized cell assay was performed using software from Persceptics Biodivision (Knoxville, TN) as described by Li *et al.* (1995)

Electron Microscopy

Log-phase cells were spun down, washed three times with water, and then resuspended in freshly prepared 2% potassium permanganate for 45 min at room temperature. Cells were then washed again in water. Pellets were processed by dehydration in a graded series of 50–100% ethanol followed by propylene oxide and embedded in Epon 812 (Taab Laboratories Equipment, Berkshire, United Kingdom). Sections were cut with a diamond knife and mounted on carbon–formvar-coated grids. Sections were stained for 4 min with a solution of Reynolds lead citrate (Reynolds, 1963), then washed and viewed with a Philips CM10 electron microscope (Cheshire, CT).

RESULTS

Sla1p Localizes to the Cortical Actin Patches

The deletion of *SLA1* causes cells to be temperature sensitive for growth and to have associated actin defects characterized by fewer and larger cortical patches (Holtzman *et al.*, 1993). To ascertain whether the effects of mutations in *SLA1* on actin organization might be direct, the subcellular localization of Sla1p was determined. Other genes, such as *ANC1*, which encodes a nuclear protein, cause actin defects when deleted, although their gene products are not localized to the actin cytoskeleton (Welch and Drubin, 1994). An antiserum was raised to amino acids 854–920 of Sla1p. After affinity purification this antiserum recognized a single protein of 148 kDa (versus a predicted molecular weight of 136 kDa) on Western blots (Figure 1A). Figure 1, B and C, shows the colocalization of Sla1p with a subset of the cortical actin patches. Colocalization of Sla1 to the actin cables was not observed. In addition, there was no detectable staining in *sla1* null cells (our unpublished results). We also generated a myc-tagged version of Sla1p, which revealed a staining pattern like that obtained with the anti-Sla1p antibodies (our unpublished results). The fluorescence data demonstrate that Sla1p is well positioned to be playing a direct role in the organization of actin assembly at the yeast cell cortex.

Localization of Actin-associated Proteins in the Absence of Sla1p

Many proteins show complete or partial colocalization with cortical actin patches. Other proteins such as the Rab-GTPase Sec4p do not colocalize with actin but nevertheless depend on an intact actin cytoskeleton to achieve a polarized localization at the presumptive bud site and in the bud of growing cells. To explore the possible role of Sla1p in the localization of such proteins, 11 cortex-associated proteins were localized

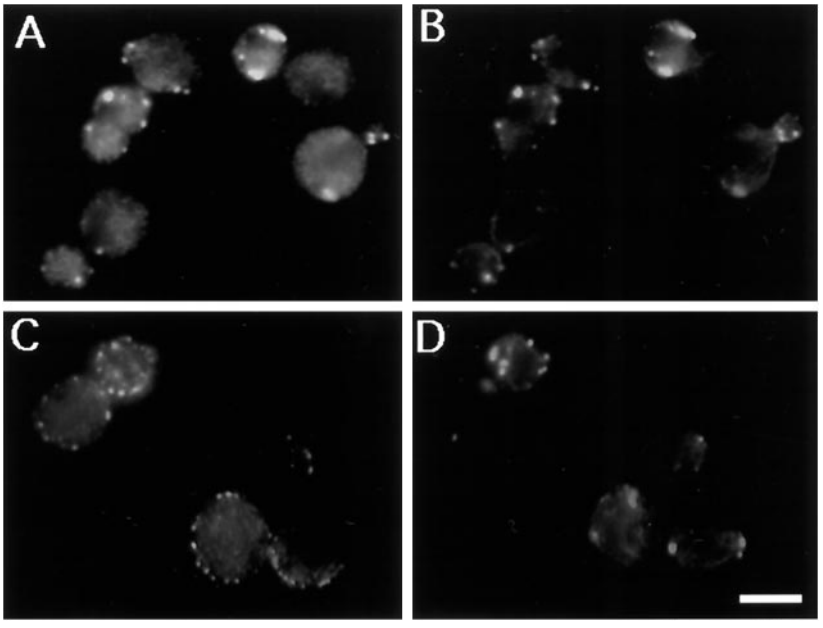

Figure 2. Localization of proteins in the absence of Sla1p. *sla1* null cells were grown to log phase and examined by double-label immunofluorescence microscopy. (A and B) Cells labeled for Abp1p (A) and actin (B). (C and D) Cells stained for Sla2p (C) and actin (D). Bar, 5 μm.

along with actin in wild-type and *sla1* null cells. Of the proteins tested that are known to bind to actin or that show significant colocalization with actin, most continued to do so even when the actin lost its wild-type "patch" structure in *sla1* null cells. This category included Abp1p, Sac6p, cofilin, Srv2p, Arp2p, and Las17p/Bee1p (Drubin *et al.*, 1988; Moon *et al.*, 1993; Freeman *et al.*, 1996; Moreau *et al.*, 1996; Li, 1997), as illustrated in Figure 2, A and B, for Abp1p. In addition, three proteins (Cdc42p, calmodulin, and Spa2p) that are highly polarized in cells but do not colocalize with actin (Snyder, 1989; Brockerhoff and Davis, 1992; Ziman *et al.*, 1993) localized normally in the absence of Sla1p (our unpublished results). In contrast, two other proteins showed significant alterations in their localization in *sla1* null cells. Sla2p, which has a C-terminal region with homology to talin (Holtzman *et al.*, 1993; Raths *et al.*, 1993) and binds actin in vitro (McCann and Craig, 1997), and which shows substantial colocalization with cortical actin patches in vivo (Yang, Cope, and Drubin, unpublished observations), does not colocalize with actin in the absence of Sla1p. Rather than associating with the actin chunks in *sla1* null cells, Sla2p is found in small patches at the cell periphery (Figure 2, C and D). In addition, Sla2p is not so well polarized in the absence of Sla1p as it is in wild-type cells. The penetrance of the Sla2p/cortical actin patch noncolocalization phenotype was assessed by counting 100 cells in each of three costaining experiments. In wild-type cells the Sla2p patches showed colocalization with a subset of actin patches in 88% of cells counted. In cells in which Sla1p was not expressed, however, only 24% of cells showed colocalization of Sla2p patches with cortical actin structures. It should be noted, however, that endocytosis, which requires Sla2p (Raths *et al.*, 1993) is not severely affected in Δ*sla1* cells (Ayscough, unpublished observation).

The second protein found to localize aberrantly in the absence of Sla1p is Rho1p. Antibodies raised and affinity-purified against a Rho1p peptide (see MATERIALS AND METHODS) recognized a protein of the appropriate size by Western blotting, and preincubation of the antibodies with the peptide blocked this recognition (Figure 3A). In addition, this band increased in intensity when *RHO1* was overexpressed (Figure 3B). When the antibodies were used for immunolocalization in wild-type cells, Rho1p was found in a patch at the site where bud emergence will occur, at the tip of the new bud, and then around the cortex of the bud as it grows (Figure 3C), as described previously (Yamochi *et al.*, 1994). In the absence of Sla1p, although Rho1p localization was relatively normal during bud formation, many unbudded cells showed staining all over the cell cortex (Figure 3D). In contrast, in wild-type cells, little or no general cortical staining was apparent in unbudded cells (Figure 3C). Counts showed that nearly 50% of unbudded *sla1* null cells showed inappropriate cortical staining (Figure 3E).

Previously we showed that in the presence of the actin-disrupting drug latrunculin-A, Sla1p was able to localize to the cell cortex but was unable to polarize to the incipient bud site (Ayscough *et al.*, 1997). The result presented here showing a dependence of Rho1p on Sla1p for its localization would suggest that Rho1p should also be unable to polarize in the absence of an intact actin cytoskeleton. We tested the dependence

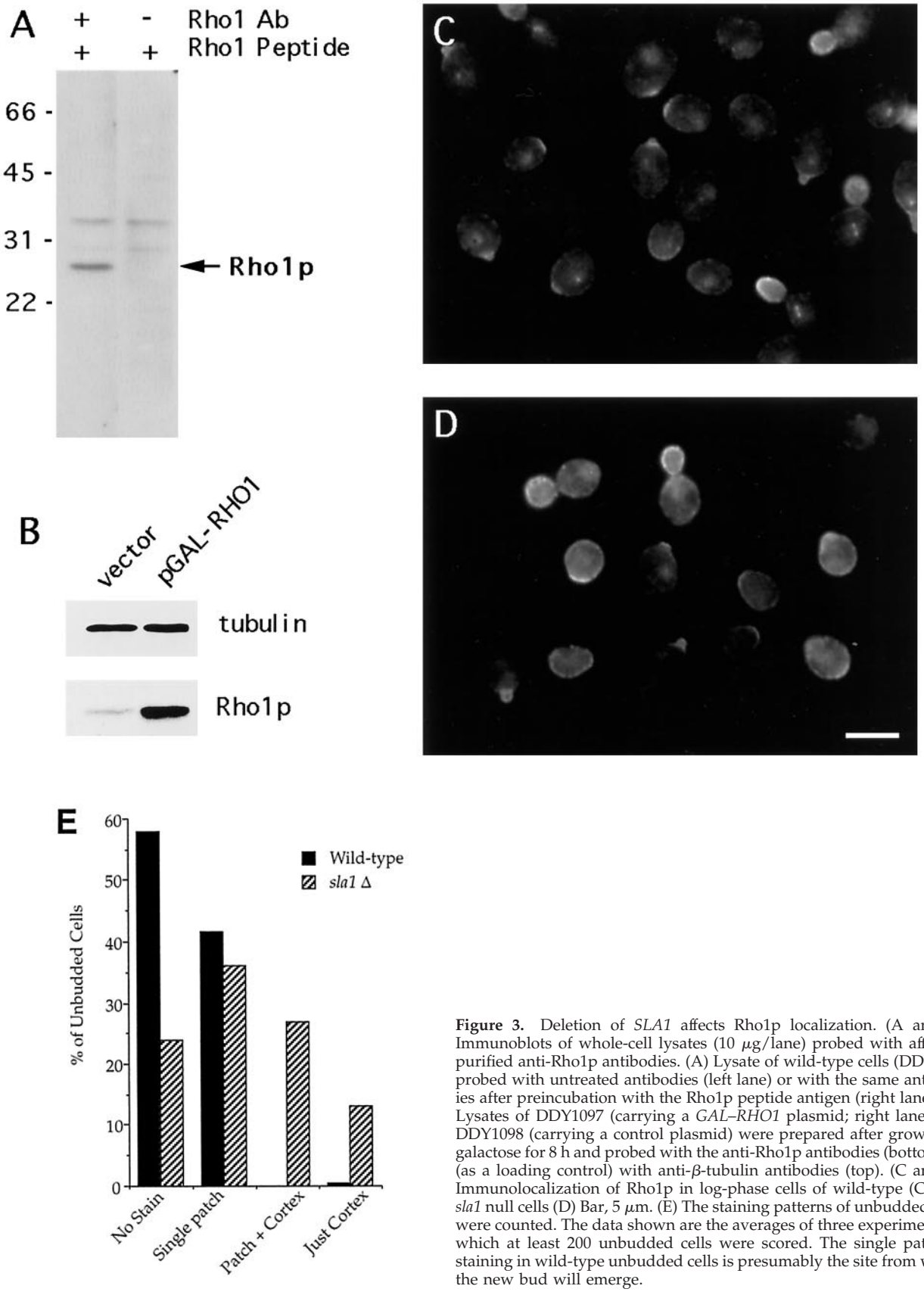

Figure 3. Deletion of *SLA1* affects Rho1p localization. (A and B) Immunoblots of whole-cell lysates (10 μg/lane) probed with affinity-purified anti-Rho1p antibodies. (A) Lysate of wild-type cells (DDY664) probed with untreated antibodies (left lane) or with the same antibodies after preincubation with the Rho1p peptide antigen (right lane). (B) Lysates of DDY1097 (carrying a *GAL–RHO1* plasmid; right lane) and DDY1098 (carrying a control plasmid) were prepared after growth on galactose for 8 h and probed with the anti-Rho1p antibodies (bottom) or (as a loading control) with anti-β-tubulin antibodies (top). (C and D) Immunolocalization of Rho1p in log-phase cells of wild-type (C) and *sla1* null cells (D) Bar, 5 μm. (E) The staining patterns of unbudded cells were counted. The data shown are the averages of three experiments in which at least 200 unbudded cells were scored. The single patch of staining in wild-type unbudded cells is presumably the site from which the new bud will emerge.

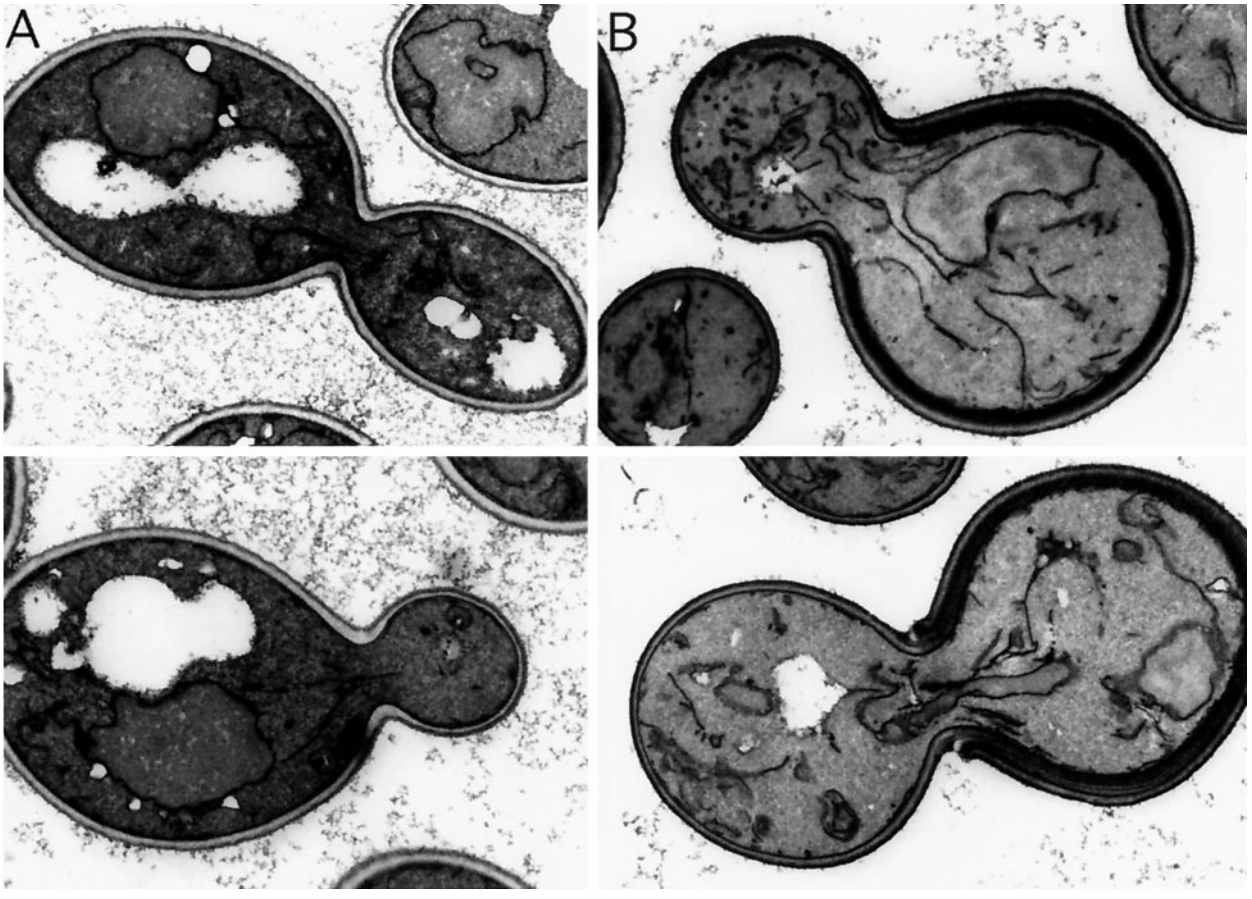

Figure 4. sla1 null cells have thick cell walls. (A) Wild-type and (B) Δ*sla1* cells were grown to log phase and then fixed and processed for electron microscopy using potassium permanganate fixation to enhance visualization of the cell wall and membranes.

of Rho1p localization on F-actin as described in Ayscough *et al.* (1997) and observed that Rho1p was able to localize to the cell cortex in the presence of latrunculin-A but was not polarized to the ends of the cell (our unpublished results). A count of the cells revealed that >70% of cells showed cortical but nonpolarized staining of Rho1p and 13% showed staining both over the entire cortex and at a patch at one end of a cell. The remaining cells showed no detectable staining for Rho1p.

Rho1p regulates the cell wall-synthesizing enzyme 1,3-β-glucan synthase (Drgonová *et al.*, 1996; Qadota *et al.*, 1996). To investigate whether the abnormal localization of Rho1p in *sla1* null cells affected cell-wall deposition, we used electron microscopy. As shown in Figure 4, the *sla1* null mutant cells showed an aberrant thickening of the walls of unbudded and mother cells. This thickening appeared to be uniform over the entire surface of the unbudded and mother cells but did not extend into the buds (Figure 4B), consistent with the relatively normal localization of Rho1p in budding cells (see above).

Expression of Mutant Forms of Sla1p Defines Functional Domains within the Protein

The primary sequence of Sla1p suggests that there are structural elements within the protein that could be responsible for specific functions and interactions. A series of *sla1* deletion mutants (Figure 5) were expressed in *sla1* null cells to explore this possibility. Western blots verified that similar levels of Sla1p were expressed in cells carrying the different constructs (our unpublished results), indicating that the stabilities of the mutant Sla1 proteins were not significantly decreased.

We then determined whether the mutant Sla1 proteins were able to rescue two phenotypes associated with the deletion of *SLA1*, temperature-sensitive growth, and Abp1p dependence. Transformants were plated onto appropriate selective media at 25° or 37°C (Figure 6A). All but one of the constructs, Sla1-ΔG1+SH3#3, were able to rescue the temperature sensitivity of the *sla1* null mutant. This construct lacked the region between the second and third SH3 domains (Gap1) and also the third

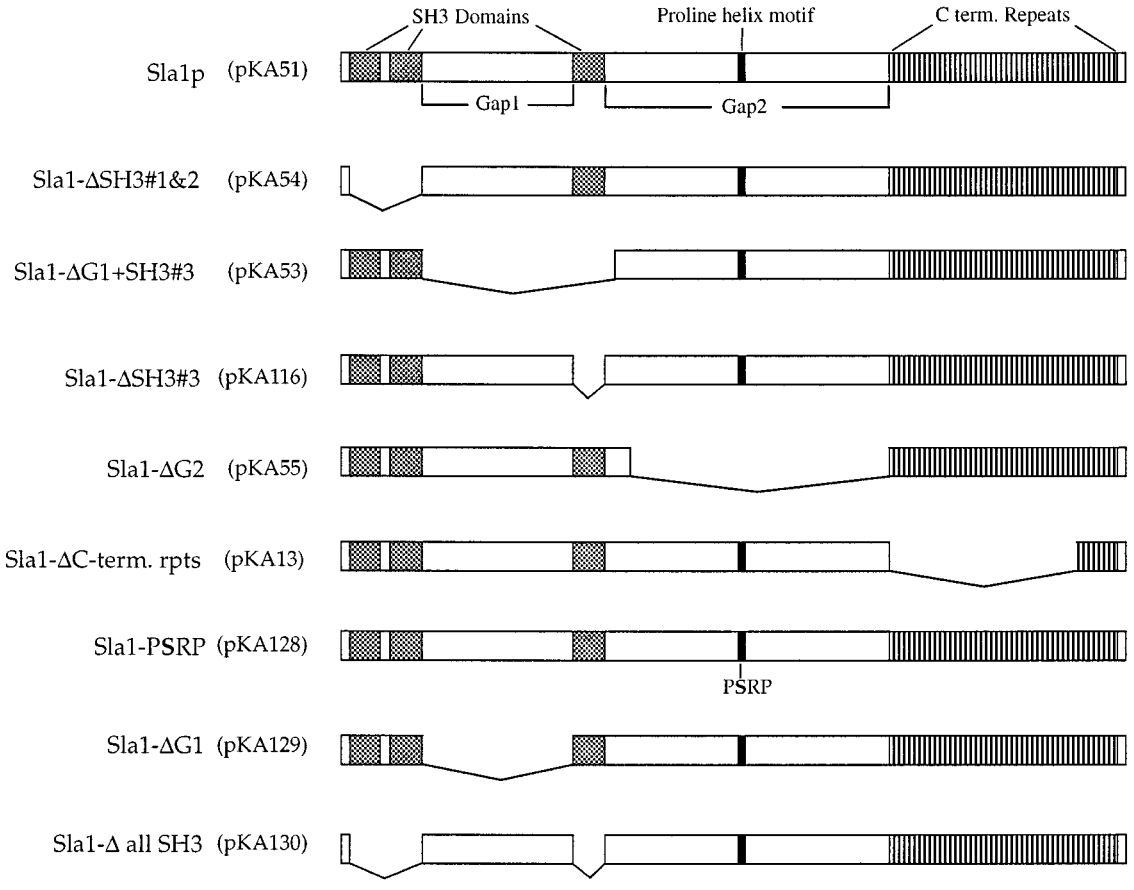

Figure 5. Mutant *sla1* constructs. Details of plasmid construction are given in Table 2.

SH3 domain (Figure 5). Interestingly, mutants lacking Gap1 alone or the third SH3 domain alone were able to support growth at the nonpermissive temperature. In addition, one other construct, Sla1-ΔG2, supported only poor growth at 37°C.

Rescue of the Abp1p-dependence phenotype was tested by plating *sla1 abp1* double-mutant cells that carried a *URA3*-marked *ABP1* plasmid and expressed the various *sla1* mutant constructs onto 5-FOA–containing medium, which selects against the *ABP1*-bearing plasmid (Figure 6B). In these cells, *ABP1* was present only on a *URA3*-marked plasmid. In the absence of Sla1p these cells cannot grow without the *ABP1* plasmid and as a result cannot grow on 5-FOA plates. Of the mutant forms of Sla1p, only cells expressing Sla1-ΔC-terminal repeats failed to rescue the Abp1p dependence. This result suggests that this repeat region is involved in a function that is redundant with that of Abp1p.

In this initial analysis, we had identified one mutant protein that rescued the Abp1p dependence of the *sla1* null mutant but not its temperature sensitivity and a second that rescued the temperature sensitivity but not the Abp1p dependence. To test whether the two Sla1p functions could be performed in transformants, the two mutant constructs were cotransformed into *sla1* null cells. The transformants grew very poorly at 37°C (Figure 6C), suggesting that Sla1-ΔG1+SH3#3 competitively inhibits Sla1-ΔC-terminal repeats (Sla1-ΔC-term.rpts).

Actin Organization in Cells Expressing the Mutant Forms of Sla1p

As mentioned above, *sla1* null mutants have fewer cortical actin patches, and these patches appear larger and less polarized than normal (Figure 7, B and C). To assess whether this aberrant actin phenotype can be attributed to a particular domain of Sla1p, we stained cells expressing the different Sla1p mutants with Rd–phalloidin. Cells with wild-type or aberrant cortical actin patches were counted, and this is summarized in Figure 7A. Representative cells for three of the mutants are depicted in Figure 7, D–F. Cells expressing

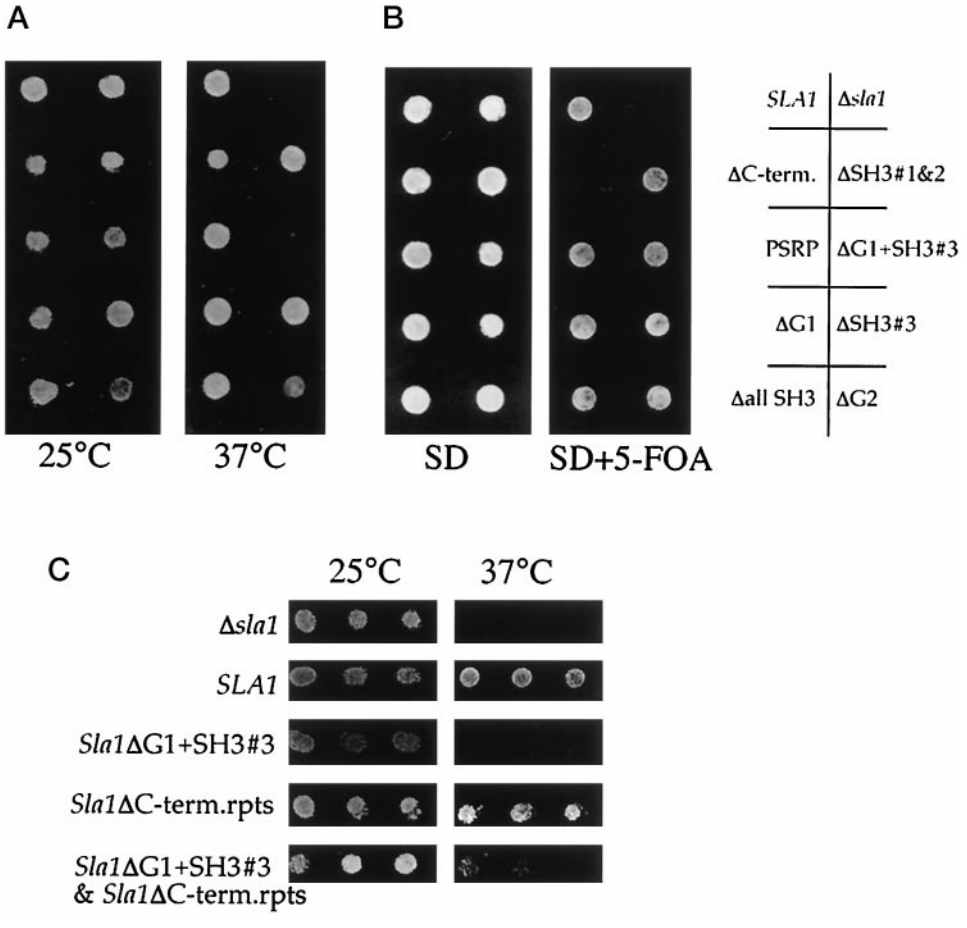

Figure 6. Growth of cells containing mutant Sla1 proteins. (A) Cells in which the genomic copy of *SLA1* was deleted (KAY14) were transformed with the *sla1* mutant constructs and plated onto selective medium at 25° and 37°C. (B) Cells carrying *ABP1* on a *URA3*-marked plasmid (KAY78) were transformed with the *sla1* mutant constructs and tested for growth on selective medium in the presence or absence of 5-FOA. (C) Cells (KAY14) were cotransformed with *sla1* mutant constructs Sla1-ΔC-term.rpts and Sla1ΔGap1+SH3#3 and tested for growth at 37°C. Expression of both forms of Sla1p was verified by Western blotting.

Sla1-ΔG1+SH3#3 (Figure 7D) had the most severe actin phenotype, similar to that in *sla1* null cells, indicating that this domain plays a critical role in regulation of cortical actin organization. In contrast, cells expressing most of the other mutant forms of Sla1p had a staining pattern almost indistinguishable from that of wild-type cells. For example, Figure 7E shows the staining pattern for Sla1-ΔC-terminal repeats. Thus, these proteins contain the information necessary for maintaining normal cortical actin cytoskeleton organization. Some of the mutants, including Sla1-ΔSH3#1&2 and Sla1-ΔGap1, have a partially penetrant actin phenotype with ~15–20% of cells in the population having actin chunks, although the remaining cells have a wild-type actin appearance (Figure 7F, Sla1-ΔSH3#1&2).

We also performed double-labeling immunofluorescence microscopy for actin and Sla2p in cells expressing mutant forms of Sla1p (our unpublished results). Our results indicated that uncoupling of Sla2p and cortical actin patch localization correlates with the severity of the actin defect rather than a specific Sla2p-binding domain in Sla1p.

Analysis of the Role of Sla1p Using a Permeabilized Cell Assay

An in vitro permeabilized cell assay was used to test further the role of Sla1p in the regulation of actin patch assembly. The assay measures the nucleated assembly of exogenously added rhodamine–actin into polarized patches at the cortex of permeabilized cells (Li *et al.*, 1995). These patches resemble those observed in vivo in terms of their size and distribution (Figure 8A). As reported previously (Li *et al.*, 1995), permeabilized *sla1* null cells are incapable of supporting nucleated actin assembly and display only a low background level of rhodamine–actin fluorescence that is never assembled into cortical patches (Figure 8B). *sla1* null cells expressing three of the mutant *sla1* constructs were examined, and the data were quantified and expressed as the range of fluorescence intensities measured within the buds of small-budded cells. Cells expressing Sla1-ΔSH3#1&2 or Sla1-ΔC-terminal repeats assembled distinct polarized patches of rhodamine–actin resembling those seen in wild-type cells, and the levels of fluorescence were similar to, or (for

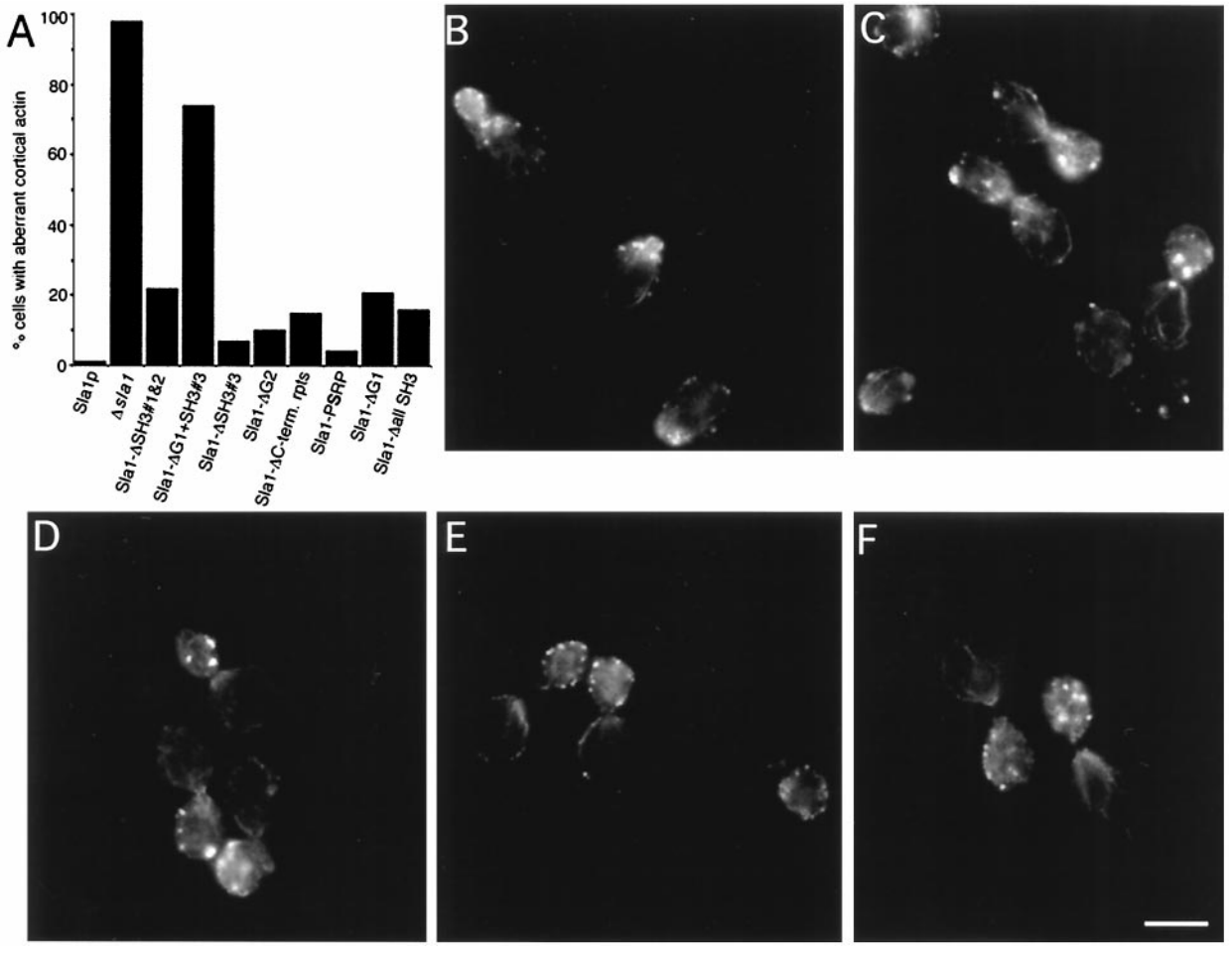

Figure 7. Actin organization in cells expressing mutant forms of Sla1p. Log-phase cells were processed for Rd–phalloidin staining. (A) For each mutant at least 300 cells were scored for wild-type or aberrant actin patch morphology. Representative images of actin staining are shown for cells expressing (B) wild-type Sla1p, (C) no Sla1p, (D) Sla1-ΔG1+SH3#3, (E) Sla1-ΔC-terminal repeats, (F) Sla1-ΔSH3#1&2. Bar, 5 μm.

Sla1-ΔSH3#1&2) somewhat greater than, those observed in wild-type cells (Figures 8, C and E).

In contrast, deletion of the Gap1 region and third SH3 domain together, but of neither alone, caused cells to be fully defective in the incorporation of rhodamine–actin into cortical actin structures (Figure 8D).

To investigate further the importance of Sla1p in the assembly of actin patches, cell extracts were added back to permeabilized *sla1* null cells in an attempt to reconstitute the actin-assembly activity. The activity could indeed be restored by the addition of wild-type cell extracts, but extracts from *sla1* null cells or from cells expressing only Sla1-ΔG1+SH3#3 were not able to restore the actin-assembly activity (Eby and Ayscough, unpublished data; see MATERIALS AND METHODS). These data lend further support to the conclusion that Sla1p plays a direct role in regulation of the cortical actin cytoskeleton.

A Fission Yeast Homologue of SLA1 Can Rescue the Temperature Sensitivity of S. cerevisiae sla1 Null Cells

A full-length homologue of *SLA1* was identified in the *S. pombe* genome database. Although the overall sequence similarity is not high (27%), the predicted *S. pombe* protein contains the same recognizable domains of Sla1p, including three SH3 domains, a proline helix motif, and a C-terminal repeat region (Figure 9A). In addition, in the central third of the proteins were two unrelated regions, each of ~60 amino acids, that were more similar (58 and 60% identity, respectively) than any other part of the protein (Figure 9A). These domains do not share significant homology with other sequences in the publicly accessible databases. The antisera raised to *S. cerevisiae* Sla1p did not recognize a protein of the appropriate size on a Western blot of

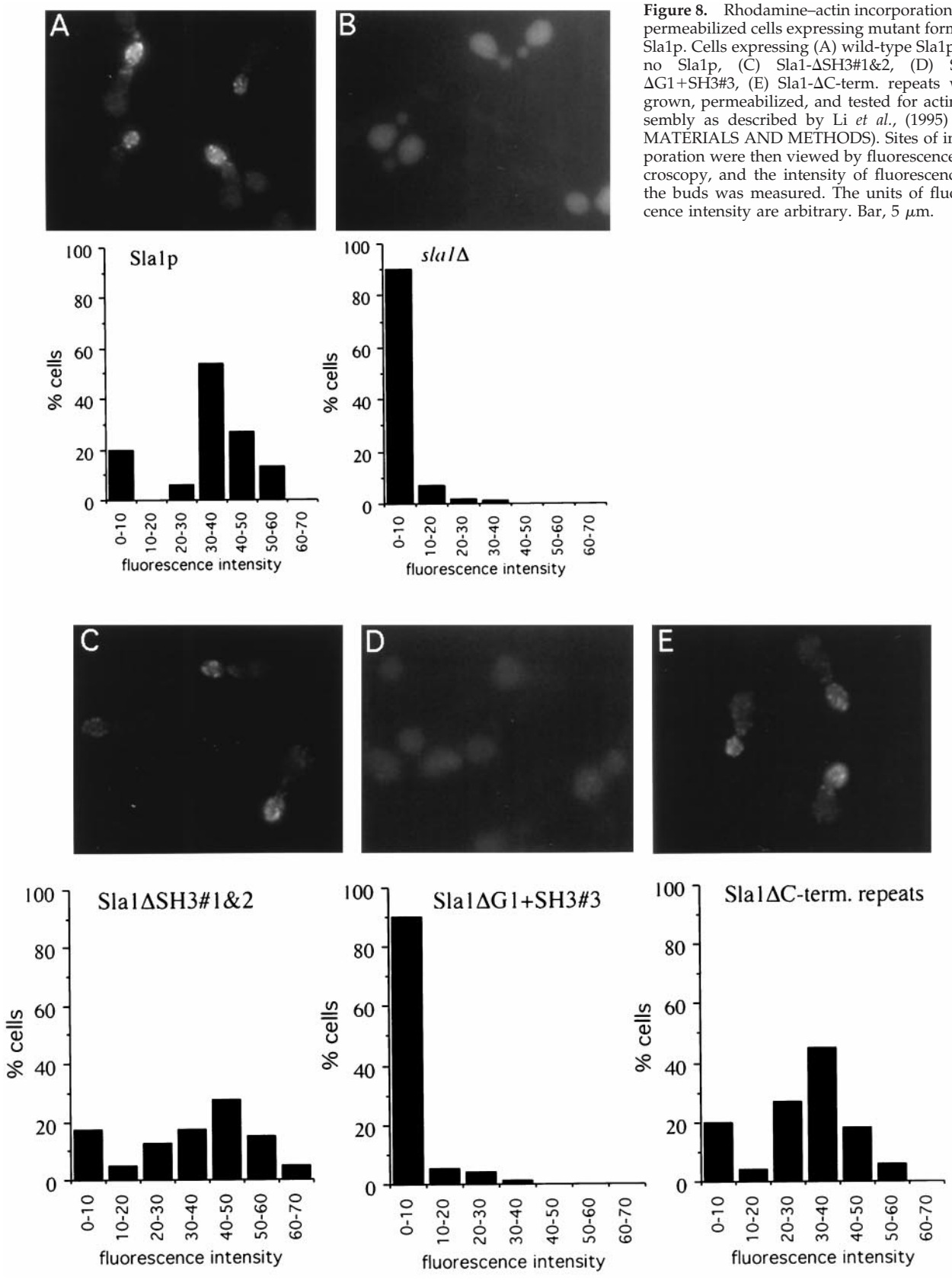

Figure 8. Rhodamine–actin incorporation into permeabilized cells expressing mutant forms of Sla1p. Cells expressing (A) wild-type Sla1p, (B) no Sla1p, (C) Sla1-ΔSH3#1&2, (D) Sla1-ΔG1+SH3#3, (E) Sla1-ΔC-term. repeats were grown, permeabilized, and tested for actin assembly as described by Li *et al.*, (1995) (see MATERIALS AND METHODS). Sites of incorporation were then viewed by fluorescence microscopy, and the intensity of fluorescence in the buds was measured. The units of fluorescence intensity are arbitrary. Bar, 5 μm.

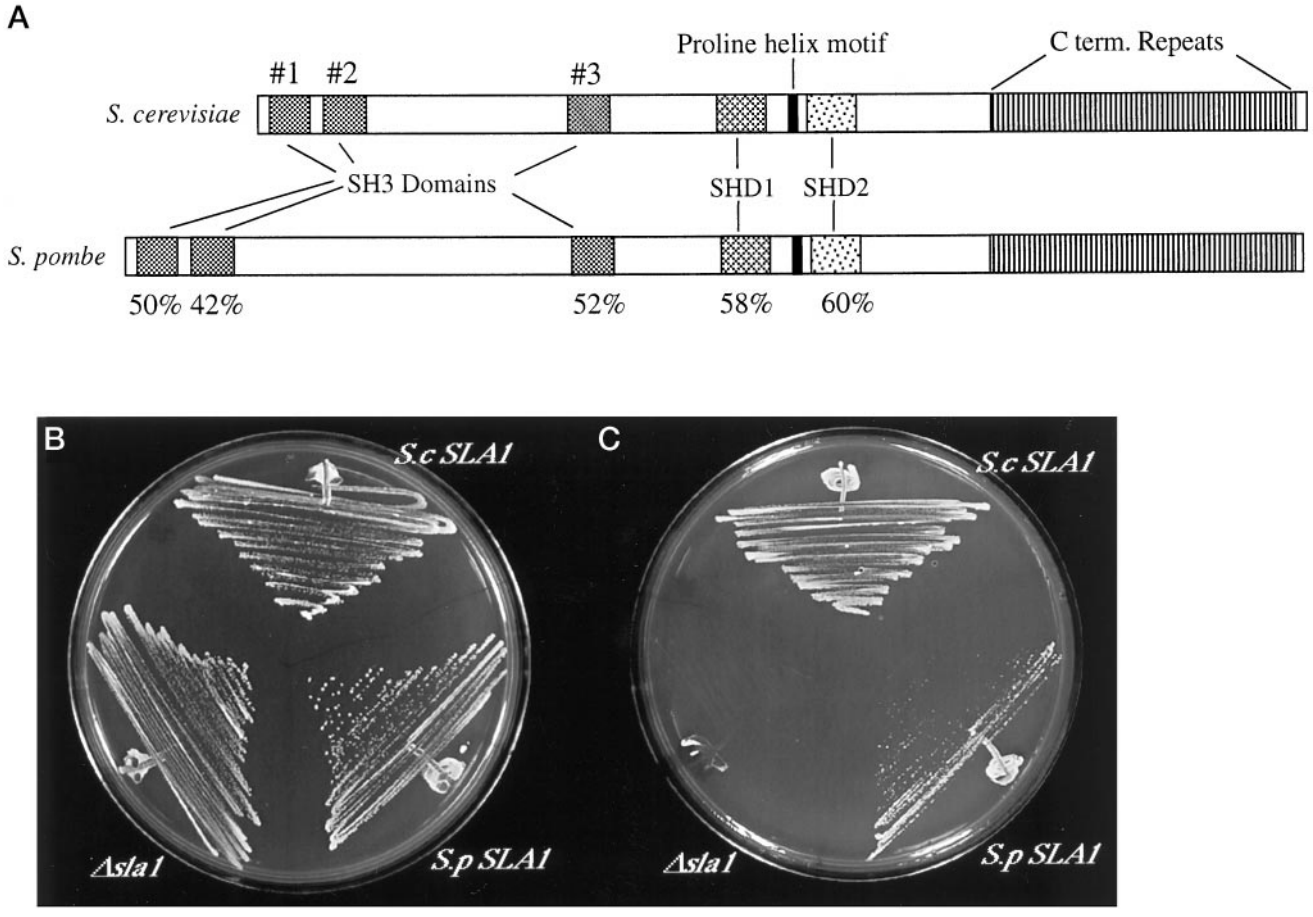

Figure 9. The *S. pombe* homologue of *SLA1* rescues the temperature sensitivity of *S. cerevisiae sla1*Δ cells. (A) *S. pombe* Sla1p has a domain structure similar to that of *S. cerevisiae* Sla1p. Two regions of high homology are designated SHD (Sla1p homology domain) 1 and 2. The percentages of identity of the SH3 domains and the SHD regions are noted beneath the respective motifs. Growth of *S. cerevisiae sla1* null cells (KAY14) containing *S. cerevisiae SLA1*, *S. pombe sla1*, or vector alone was tested at (B) 29°C and (C) 37°C.

S. pombe proteins, nor did they give a distinct staining pattern by immunofluorescence. The *S. pombe sla1* gene was cloned from cosmid DNA into an overexpression vector and transformed into *S. cerevisiae* cells in which *SLA1* had been deleted. The *S. pombe* gene was able to partially rescue the temperature sensitivity associated with the deletion (Figure 9, B and C); however, staining of these cells for actin indicated that their aberrant actin organization was not rescued by the fission yeast gene.

DISCUSSION

Interactions with Cortical Proteins

Regulation of the structure and organization of the cortical actin cytoskeleton is essential for many processes in eukaryotes, including the chemotactic responses of *Dictyostelium* and neutrophils, differentiation of epithelial and neuronal cells, and budding and mating projection formation in yeast. The high level of conservation among proteins that associate with and regulate actin organization suggests that gaining an understanding of these processes in genetically manipulable yeast cells might facilitate our understanding of the cytoarchitecture of more complex eukaryotic organisms. In this study, we have shown that a protein, Sla1p, associates with the cortical actin cytoskeleton. As observed previously, deletion of the *SLA1* gene disrupts the wild-type organization of cortical actin, and instead, staining with Rd–phalloidin reveals fewer, larger chunks of actin (Holtzman *et al.*, 1993). Because Sla1p is normally localized with cortical actin, we believe that this might indicate that it has a specific role in regulating the structure of the cortical patches. It has also been noted previously that *sla1* null cells are more resistant to the effects of the actin-disrupting drug latrunculin-A (Ayscough *et al.*, 1997). Thus, we postulate that actin in Δ*sla1* cells is in some

way either less dynamic or more stable than in the wild-type situation. Thus, the presence of Sla1p may increase actin dynamic turnover by recruiting or facilitating interaction of depolymerizing or destabilizing proteins, or alternatively, it might limit access of stabilizing proteins to actin. An argument against the possibility that Sla1p recruits depolymerizing factors is our observation that the major actin depolymerizing protein in yeast cells, cofilin, continues to associate with cortical actin structures in the absence of Sla1p (our unpublished results).

To further our understanding of the role of Sla1p, we analyzed, in *sla1* null cells, the localization of other proteins associated specifically with the bud cortex. We observed that two proteins become aberrantly localized in the absence of Sla1p. One of these, Sla2p, normally shows substantial colocalization with the actin cytoskeleton (Yang, Cope, and Drubin, unpublished observations). *SLA2* was first identified in yeast as a gene that interacts with *ABP1* and also as a gene, *END4*, that when mutated caused a defect in endocytosis (Holtzman *et al.*, 1993; Raths *et al.*, 1993). Homologues of Sla2p have been identified in both *Caenorhabditis elegans* and human cells (Kalchman *et al.*, 1997), and the human protein has been demonstrated to associate with actin in vitro (McCann and Craig, 1997). In the absence of Sla1p, however, there is almost no colocalization of Sla2p and cortical actin patches. The fact that Sla2p is able to localize to small patch-like structures at the cell cortex in the absence of similar actin patches, however, suggests that the Sla2p interacts with proteins other than actin at the cell cortex and that Sla1p might be involved in facilitating the interaction between Sla2p-containing patches and the cortical actin patches. One consequence of the absence of this interaction is that Sla2p does not polarize as well as in wild-type cells. Interestingly, *sla1* null cells are not severely affected in endocytosis, indicating that the association of Sla2p patches with the actin patches is not a critical interaction for this function in yeast. This result is somewhat paradoxical because actin is required for endocytosis (Kübler and Riezman, 1993). A possibility is that the role of actin in endocytosis is more regulatory and that actin must be released from proteins mediating endocytosis for the process to occur.

The second protein that shows mislocalization in *sla1* null cells is Rho1p. We hypothesize that the mislocalization of Rho1p in unbudded cells produces a novel phenotype in which mother cells have thick cell walls and generate daughter cells with apparently normal cell walls. Our data indicate that the Rho1p mislocalization occurs largely during the unbudded part of the cell cycle. Other observations, however, suggest that this mislocalization is not due to *sla1* null cells being delayed in the G1 part of the cell cycle, because comparison of log-phase cultures of wild-type and *sla1* null strains show that both have similar proportions of unbudded and budded cells. In addition, FACS analysis indicates that a similar proportion of *sla1* null and wild-type cells in an asynchronous population are in G1 and G2 (Ayscough, unpublished data). In both mammalian cells and *S. cerevisiae*, SH3 domain-containing proteins have been reported to associate with Rho–GAP proteins (Cicchetti *et al.*, 1992; Bender *et al.*, 1996). One possibility therefore is that one or more of the SH3 domains in Sla1p interacts with a Rho–GAP. This Rho–GAP might then be responsible for maintaining Rho1p in an inactive state such that cell wall synthesis does not occur at inappropriate times or places in the cell. In the absence of Sla1p, the Rho–GAP itself might become mislocalized, abrogating its normal interaction with Rho1p. This might allow Rho1p to be inappropriately activated such that cell wall is synthesized during early G1-phase. Later in G1, cell polarity determinants such as Cdc42p and Bem1p are still able to localize normally to the incipient bud site, and Rho1p can presumably still make the correct interactions with this complex before and after bud emergence. Future experiments will examine the role of specific SH3 domains in Rho1p localization, and will also aim to determine whether any of the Rho–GAPs identified in *S. cerevisiae* associate with Sla1p.

Sla1p Domain Structure

The generation of a number of mutants with deletions in *SLA1* allowed us to associate different functions of Sla1p with different parts of the Sla1p primary sequence. Most notably, the region from the second SH3 domain to just C-terminal of the third SH3 domain is important for the role of Sla1p in generating normal actin organization. Mutants expressing a form of Sla1p lacking this region are temperature sensitive, have an in vivo actin phenotype similar to that of the *sla1* deletion strain, and are defective in the permeabilized cell actin assembly assay. This mutant Sla1p, however, is able to rescue the *ABP1* phenotype associated with the *sla1* deletion, indicating that it contains domains important for this other function. Deletion of both the Gap1 region and the SH3#3 is necessary for this phenotype because deletion of either domain alone produces a protein that can rescue all assessed phenotypes. Deletion of the C-terminal repeats, in contrast, results in a protein capable of rescuing the actin phenotype but not the *ABP1* dependency. The *ABP1* dependency cannot be rescued if the repeats are expressed alone (our unpublished results), perhaps because they do not contain sufficient information to localize this domain correctly in cells. Sla1p contains 26 repeats with the approximate consensus TGGXXXPQ, in which X residues are most often aliphatic. Although secondary structure predictions fail

to reveal an obvious structure for these repeats, it has been noted in wheat glutenins and barley hordeins that seven to nine amino acid repeats rich in glycine, proline, and glutamine can form a rod-like structure composed of regular β-turns (Field *et al.*, 1987; Halford *et al.*, 1992). Therefore, this region of Sla1p might have a similar structure. Interestingly, the *S. pombe* homologue of *SLA1* has repeats at its C-terminus that are rich in similar residues, but with a consensus of only six to seven amino acids (TGXXPQ(X)).

The identification of a homologue of *SLA1* in *S. pombe* allows us to determine the parts of the protein that have been most highly conserved. Like its *S. cerevisiae* counterpart, *S. pombe* Sla1p has three SH3 domains with a gap between the second and third of these domains. The fact that each SH3 domain is more highly related to the corresponding SH3 domain in the homologous protein than they are to one another suggests that the domains have specific functions and possibly that the interactions they make are also conserved. We were also able to identify two other domains that are highly conserved between the two proteins (SHD1 and SHD2, Figure 9A). Although not similar to one another, or to other sequences in the database, these 60 amino acid domains are the most highly conserved regions between the two Sla1 proteins. The identification of these domains will allow us to focus future studies on identifying proteins that interact specifically with these regions. In *S. cerevisiae*, deletion of both domains (in Sla1ΔGap2 mutant) leads to a slow-growth phenotype, particularly at higher temperatures.

The ability of the *S. pombe SLA1* to rescue the temperature sensitivity associated with deletion of *S. cerevisiae SLA1* indicates that at least some of the interactions that are made by this protein are conserved. Therefore, further study of these domains and their interactions will also provide insights into functioning of the actin cytoskeleton in *S. pombe* and places emphasis on determining whether *SLA1* homologues exist in other organisms.

ACKNOWLEDGMENTS

We are grateful to Doug Stirling for critical reading of this manuscript; Kim Nasmyth for the plasmid used to generate myc-tagged Las17p and Sla1p; Mike Stark, Jeff Field, Barbara Winsor, and Mike Snyder for antibodies; Doug Holtzman for initiating these studies; Rose Watson for invaluable assistance with electron microscopy; and Dr. David King for very helpful advice on peptide chemistry and antibody production. This work was supported by a Career Development Fellowship from The Wellcome Trust to K.R.A. and H.D. (050934/Z/97), and National Institutes of Health grant GM-50399 to I.H., American Cancer Society grant FRA-442 to D.G.D., T.L., and J.J.E., and a Helen Hay Whitney Fellowship to K.G.K.

REFERENCES

Ayscough, K.R. (1998). In vivo functions of actin-binding proteins. Curr. Opin. Cell Biol. *10*, 102–111.

Ayscough, K.R., and Drubin, D.G. (1997). Immunofluorescence microscopy of yeast cells. In: Cell Biology: A Laboratory Handbook, vol. 2, ed. J. Celis, San Diego: Academic Press, 477–485.

Ayscough, K.R., Stryker, J., Pokala, N., Sanders, M., Crews, P., and Drubin, D.G. (1997). High rates of actin filament turnover in budding yeast and roles for actin in establishment and maintenance of cell polarity revealed using the actin inhibitor latrunculin-A. J. Cell Biol. *137*, 399–416.

Baudin, A., Ozier-Kalogeropoulos, O., Denoul, A., Lacroute, F., and Cullin, C. (1993). A simple and efficient method for direct gene deletion in *Saccharomyces cerevisiae*. Nucleic Acids Res. *21*, 3329–3330.

Belmont, L.D., and Drubin, D.G. (1998). The yeast V159N actin mutant reveals roles for actin dynamics in vivo. J. Cell Biol. *142*, 1289–1299.

Bender, L., Lo, H.S., Lee, H., Kokojan, V., Peterson, J., and Bender, A. (1996). Associations among PH and SH3 domain-containing proteins and Rho-type GTPases in yeast. J. Cell Biol. *133*, 879–894.

Bond, J.F., Fridovich-Keil, J., Pillus, L., Mulligan, R.C., and Solomon, F. (1986). A chicken-yeast chimeric β-tubulin protein is incorporated into mouse microtubules in vivo. Cell *44*, 461–468.

Brockerhoff, S.E., and Davis, T.N. (1992). Calmodulin concentrates at regions of cell growth in *Saccharomyces cerevisiae*. J. Cell Biol. *118*, 619–629.

Cicchetti, P., Mayer, B.J., Thiel, G., and Baltimore, D. (1992). Identification of a protein that binds to the SH3 region of Abl and is similar to Bcr and GAP-rho. Science *257*, 803–806.

Drgonová, J., Drgon, T., Tanaka, K., Kollar, R., Chen, G.C., Ford, R.A., Chan, C.S.M., Takai, Y., and Cabib, E. (1996). Rho1p, a yeast protein at the interface between cell polarization and morphogenesis. Science *272*, 277–279.

Drubin, D.G., Miller, K.G., and Botstein, D. (1988). Yeast actin binding proteins: evidence for a role in morphogenesis. J. Cell Biol. *107*, 2551–2561.

Field, J., Tatham, A., and Shewry, P. (1987). The structure of a high-Mr subunit of durum wheat (*Triticum durum*) gluten. Biochem. J. *247*, 215–221.

Freeman, N.L., Lila, T., Mintzer, K.A., Chen, Z., Pahk, A.J., Ren, R., Drubin, D.G., and Field, J. (1996). A conserved proline rich region of the *Saccharomyces cerevisiae* cyclase-associated protein binds SH3 domains and modulates cytoskeletal localization. Mol. Cell. Biol. *16*, 548–556.

Gao, B., Klein, L.E., Britten, R.J., and Davidson, E.H. (1986). Sequence of mRNA coding for bindin, a species specific sea urchin sperm protein required for fertilization. Proc. Natl. Acad. Sci. USA *83*, 8634–8638.

Halford, N., Tatham, A., Sui, E., Daroda, L., Dreyer, T., and Shewry, P. (1992). Identification of a novel β-turn rich repeat motif in the D. hordeins of barley. Biochim. Biophys. Acta *1122*, 118–122.

Holtzman, D.A., Yang, S., and Drubin, D.G. (1993). Synthetic-lethal interactions identify two novel genes, *SLA1* and *SLA2*, that control membrane cytoskeleton assembly in *Saccharomyces cerevisiae*. J. Cell Biol. *122*, 635–644.

Kaiser, C., Michaelis, S., and Mitchell, A. (1994). Methods in Yeast Genetics: A Laboratory Course Manual, Cold Spring Harbor, NY: Cold Spring Harbor Laboratory Press.

Kalchman, M.A., *et al.* (1997). HIP1, a human homologue of *S. cerevisiae* Sla2p, interacts with membrane-associated huntingtin in the brain. Nature Genet. *16*, 44–53.

Kübler, E., and Riezman, H. (1993). Actin and fimbrin are required for the internalization step of endocytosis in yeast. EMBO J. *12*, 2855–2862.

Li, R. (1997). Bee1, a yeast protein with homology to Wiscott-Aldrich Syndrome Protein, is critical for the assembly of cortical actin cytoskeleton. J. Cell Biol. *136*, 649–658.

Li, R., Zheng, Y., and Drubin, D. (1995). Regulation of cortical actin cytoskeleton assembly during polarized cell growth in budding yeast. J. Cell Biol. *128*, 599–615.

Mayer, B., and Eck, M. (1995). Minding your P's and Q's. Curr. Biol. *5*, 364–367.

McCann, R.O., and Craig, S.W. (1997). The I/LWEQ module: a conserved sequence that signifies F-actin binding in functionally diverse proteins from yeast to mammals. Proc. Natl. Acad. Sci. USA *94*, 5679–5684.

Minor, J.E., Fromsen, D.R., Britten, R.J., and Davidson, E.H. (1991). Comparison of bindin proteins of *Strongylocentrus franciscanus*, *S. purpuratus* and *Lytechinus variegatus*: sequences involved in the species specificity of fertilization. Mol. Biol. Evol. *8*, 781–795.

Moon, A.L., Janmey, P.A., Louie, A., and Drubin, D.G. (1993). Cofilin is an essential component of the yeast cortical actin cytoskeleton. J. Cell Biol. *120*, 421–435.

Moreau, V., Madania, A., Martin, R., and Winsor, B. (1996). The *Saccharomyces cerevisiae* actin related protein Arp2 is involved in the actin cytoskeleton. J. Cell Biol. *134*, 117–132.

Pawson, T., and Gish, G.D. (1992). SH2 and SH3 domains: from structure to function. Cell *71*, 359–362.

Pringle, J., Adams, A., Drubin, D., and Haarer, B. (1991). Immunofluorescence methods for yeast. Methods Enzymol. *194*, 565–602.

Pringle, J.R., Preston, R.A., Adams, A.E.M., Stearns, T., Drubin, D.G., Haarer, B.K., and Jones, E.W. (1989). Fluorescence microscopy methods for yeast. Methods Cell Biol. *31*, 357–435.

Qadota, H., Python, C.P., Inoue, S.B., Arisawa, M., Anraku, Y., Watanabe, T., Levin, D.E., and Ohya, Y. (1996). Identification of yeast rho1p GTPase as a regulatory subunit of 1,3-β-glucan synthase. Science *272*, 279–281.

Raths, S., Rohrer, J., Crausaz, F., and Riezman, H. (1993). *end3* and *end4*: two mutants defective in receptor-mediated endocytosis in *Saccharomyces cerevisiae*. J. Cell Biol. *120*, 55–65.

Ren, R., Mayer, B.J., Cicchetti, P., and Baltimore, D. (1993). Identification of a ten-amino acid proline-rich SH3 binding site. Science *259*, 1157–1161.

Reynolds, E.S. (1963). The use of lead citrate at high pH as an electron-opaque stain in electron microscopy. J. Cell Biol. *17*, 208–212.

Sikorski, R.S., and Hieter, P. (1989). A system of shuttle vectors and yeast host strains designed for efficient manipulation of DNA in *Saccharomyces cerevisiae*. Genetics *122*, 19–27.

Snyder, M. (1989). The *SPA2* protein of yeast localizes to sites of cell growth. J. Cell Biol. *108*, 1419–1429.

Sorger, P.K., and Pelham, H.R. (1987). Purification and characterization of a heat-shock element binding protein from yeast. EMBO J. *6*, 3035–3041.

Stirling, D., Welch, K., and Stark, M. (1994). Interaction with calmodulin is required for the function of Spc110p, an essential component of the yeast spindle pole body. EMBO J. *13*, 4329–4342.

Tang, H., and Cai, M. (1996). The EH-domain containing protein pan1 is required for normal organization of the actin cytoskeleton in *Saccharomyces cerevisiae*. Mol. Cell. Biol. *16*, 4897–4914.

Welch, M.D., and Drubin, D.G. (1994). A nuclear protein with sequence similarity to proteins implicated in human acute leukemias is important for cellular morphogenesis and actin cytoskeletal function in *Saccharomyces cerevisiae*. Mol. Biol. Cell *5*, 617–632.

Welch, M.D., Holtzman, D., and Drubin, D.G. (1994). The yeast actin cytoskeleton. Curr. Opin. Cell Biol. *6*, 110–119.

Yamochi, W., Tanaka, K., Nonaka, H., Maeda, A., Musha, T., and Takai, Y. (1994). Growth site localization of Rho1 small GTP-binding protein and its involvement in bud formation in *Saccharomyces cerevisiae*. J. Cell Biol. *125*, 1077–1093.

Yu, H., Chen, J., Feng, S., Dalgarno, D., Brauer, A., and Schreiber, S. (1994). Structural basis for the binding of proline rich peptides to SH3 domains. Cell *76*, 933–945.

Ziman, M., Preuss, D., Mulholland, J., O'Brien, J.M., Botstein, D., and Johnson, D.I. (1993). Subcellular localization of Cdc42p, a *Saccharomyces cerevisiae* GTP-binding protein involved in the control of cell polarity. Mol. Biol. Cell *4*, 1307–1316.